

## Application of Moment Interaction to the Construction of a Stable Model of Graphite Crystal Lattice

I. E. Berinskii<sup>1\*</sup>, E. A. Ivanova<sup>2\*\*</sup>, A. M. Krivtsov<sup>2\*\*\*</sup>, and N. F. Morozov<sup>1\*\*\*\*</sup>

<sup>1</sup>*Institute of Problems of Mechanical Engineering, Russian Academy of Sciences, Bol'shoy pr-t 61, St. Petersburg, 199178 Russia*

<sup>2</sup>*Saint-Petersburg State Polytechnical University, Polytekhnicheskaya 29, St. Petersburg, 195251 Russia*

Received April 6, 2007

**Abstract**—The aim of the present paper is to construct and study a model of pair moment interaction between carbon atoms in the two-dimensional graphite lattice. The carbon atom is modeled by a structure consisting of three rigidly connected mass points located at the vertices of an equilateral triangle. The interaction between mass points is described by a pair force potential, but the total interatomic interaction contains moment components owing to the finite size of the structure modeling the atom. We compute rank 4 tensors characterizing the elastic properties of the graphite crystal lattice constructed on the basis of our model. We determine lattice stability criteria depending on the number of coordination spheres taken into account. We show that this model permits one to ensure stability of the graphite lattice but significantly underestimates the transverse-to-longitudinal interatomic coupling rigidity ratio. We construct a generalized moment potential that permits one to obtain a rigidity ratio consistent with experimental data.

**DOI:** 10.3103/S0025654407050020

### 1. INTRODUCTION

A well-known problem in modeling lattices with low packing density is that the use of pair potentials for describing interatomic interactions does not always result in stable lattice models. There are two alternative approaches to resolve the issue. The first approach is based on the use of multiparticle potentials [1, 2] and itself has certain difficulties related to the complicated structure of such potentials and the large number of interaction parameters. The second approach takes into account the moment contribution into interatomic interaction. In the present paper, we consider an application of the second approach to the construction of a two-dimensional hexagonal graphite lattice in which atoms (particles) are modeled as systems of rigidly connected mass points interacting with the mass points of other particles via pair potentials. For the pair potential we take the Lennard–Jones potential, because it has a relatively simple physical interpretation. The interaction thus obtained is noncentral and consists of two components, the force component described by the force vector and the moment component described by the moment vector. As is shown later, the moment component can introduce additional transverse rigidity, which can ensure stability of the hexagonal lattice.

This study is based on the theoretical considerations presented in [3] for the case of central interaction. A generalization of these methods to the case of moment interaction is given in [4] for square lattices and [5] for hexagonal lattices. There also exist other methods for introducing additional rigidity into the system. For example, a mechanical model of a carbon nanotube was proposed in [6]. This model uses elastic rods and springs connecting the atoms to ensure stability of the system. Another approach, based on the introduction of rotational degrees of freedom for describing the moment interaction, was proposed in [7].

---

\* E-mail: berigor@mail.ru

\*\* E-mail: ivanova@ei5063.spb.edu

\*\*\* E-mail: krivtsov@nm.ru

\*\*\*\* E-mail: morozov@nm1016.spb.edu

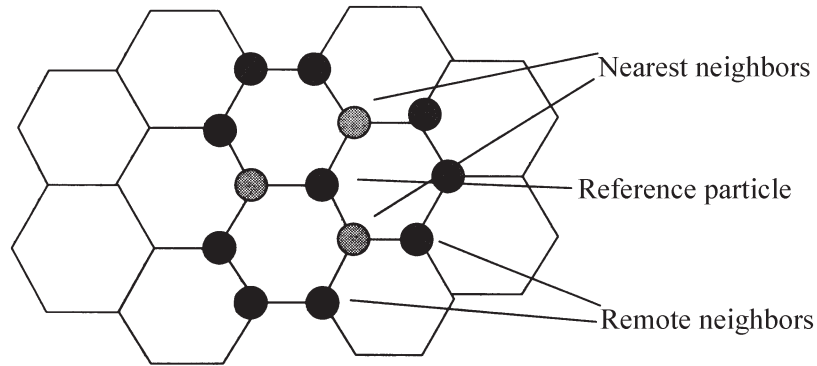


Fig. 1.

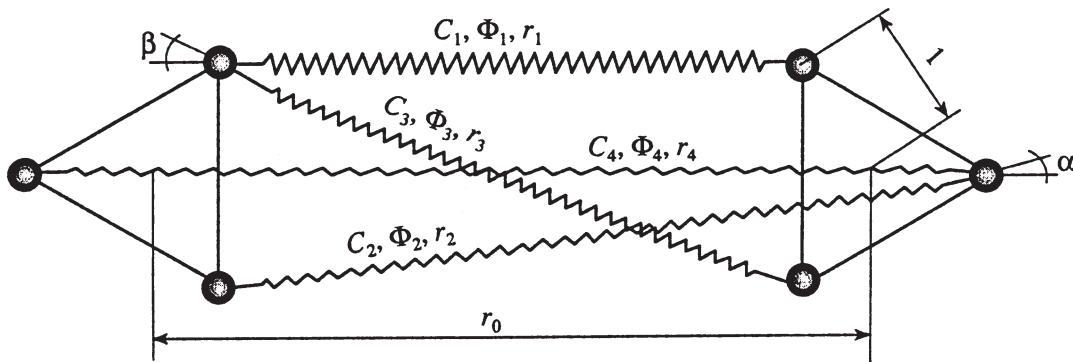


Fig. 2.

The interaction laws obtained in the present paper can be used in numerical experiments based on the molecular dynamic method. The results of this study are a step towards the construction of a universal form of the interaction potential for carbon atoms, which can be used to describe various carbon structures.

## 2. INTERACTION BETWEEN PARTICLES OF SPECIAL FORM

The graphite lattice has symmetry of order 3 (symmetry under rotation by  $2\pi/3$ ) with respect to each lattice point. The three-dimensional image of the graphite lattice structure is shown in Fig. 1. For a model of the carbon atom we take the simplest system satisfying the above symmetry, i.e., three mass points forming an equilateral triangle. The triangle is assumed to be absolutely rigid; namely, its dimensions and shape remain unchanged, but it can perform translational as well as rotational motions. Consider a system of two identical atoms—triangles whose edges face each other. The system is shown in Fig. 2. The mass points belonging to different triangles interact via pairwise central forces. For two particles, there are nine couplings between the mass points constituting these triangles. Only four of them are shown schematically by springs in Fig. 2; the other couplings can be obtained from these on the basis of the symmetry of the configuration. The corresponding distances are denoted by  $r_i$  ( $i = 1, 2, 3, 4$ ). The distance between the centers of mass of the triangles in the equilibrium configuration is denoted by  $r_0$ . We introduce the angles  $\alpha$  and  $\beta$  as shown in Fig. 2.

The interaction between the mass points forming the particles can be described by a pair interaction potential  $\Pi(r)$ . For specific computations, we use the Lennard–Jones potential

$$\Pi(r) = D \left[ \left( \frac{\rho}{r} \right)^{12} - 2 \left( \frac{\rho}{r} \right)^6 \right], \quad (2.1)$$

where  $D$  is the interaction energy and  $\rho$  is a parameter characterizing the interaction magnitude. The potential (2.1) is the simplest model interaction potential at the atomic level; it gives a good description of the asymptotics of the interatomic interaction as particles move away from each other and contains only two parameters.

The coupling rigidities  $i = 1, 2, 3, 4$  are determined by the formulas

$$C_i = \Pi''(r)|_{r=r_i}. \quad (2.2)$$

We introduce the effective particle size  $l$  equal to the distance from the center to the vertices of the triangle. Then the system in question contains three independent parameters of the dimension of length, namely, the equilibrium distance  $r_0$  between the particles, the effective particle size  $l$ , and the interaction magnitude  $\rho$ . From these parameters, we proceed to the dimensionless parameters

$$\zeta = \frac{l}{r_0} \quad (\text{the relative particle size}), \quad \eta = \frac{\rho}{r_0} \quad (\text{the relative interaction range}). \quad (2.3)$$

Using the model geometry (see Fig. 2), we obtain

$$\begin{aligned} r_1 &= r_0(1 - \zeta), & r_2 &= r_0\sqrt{1 + \zeta + \zeta^2}, \\ r_3 &= r_0\sqrt{(1 - \zeta)^2 + 3\zeta^2}, & r_4 &= r_0(1 + 2\zeta). \end{aligned} \quad (2.4)$$

The horizontal projection of the total forces acting on a particle (see Fig. 2) gives

$$2f(r_1) + 4f(r_2) \cos \alpha + 2f(r_3) \cos \beta + f(r_4) = 0. \quad (2.5)$$

Here  $f(r) = -\Pi'(r)$  is the interaction force. Equation (2.5) implies the following relation between the dimensionless parameters introduced above:

$$\eta^6 = \frac{\frac{1}{(1 - \zeta)^7} + \frac{2 + \zeta}{(1 + \zeta + \zeta^2)^4} + \frac{1 - \zeta}{[(1 - \zeta)^2 + 3\zeta^2]^4} + \frac{1}{2(1 + 2\zeta)^7}}{\frac{1}{(1 - \zeta)^{13}} + \frac{2 + \zeta}{(1 + \zeta + \zeta^2)^7} + \frac{1 - \zeta}{[(1 - \zeta)^2 + 3\zeta^2]^7} + \frac{1}{2(1 + 2\zeta)^{13}}}}. \quad (2.6)$$

### 3. STABILITY OF THE TWO-PARTICLE SYSTEM

Under the assumption that the displacements and rotations of particles are small, we represent the strain energy of the system as a quadratic form of the strains [4]:

$$U = \frac{1}{2} \boldsymbol{\varepsilon} \cdot \mathbf{A} \cdot \boldsymbol{\varepsilon} + \boldsymbol{\varepsilon} \cdot \mathbf{B} \cdot \boldsymbol{\kappa} + \frac{1}{2} \boldsymbol{\kappa} \cdot \mathbf{C} \cdot \boldsymbol{\kappa}. \quad (3.1)$$

Then the interaction force and moment are computed by the formulas

$$\mathbf{F} = \mathbf{A} \cdot \boldsymbol{\varepsilon} + \mathbf{B} \cdot \boldsymbol{\kappa}, \quad \mathbf{M} = \boldsymbol{\varepsilon} \cdot \mathbf{B} + \mathbf{C} \cdot \boldsymbol{\kappa}. \quad (3.2)$$

Here  $\boldsymbol{\varepsilon}$  and  $\boldsymbol{\kappa}$  are the strain vectors,

$$\boldsymbol{\varepsilon} \stackrel{\text{def}}{=} \mathbf{r} - \mathbf{r}_0 + \frac{1}{2} \mathbf{r}_0 \times (\boldsymbol{\varphi}_1 + \boldsymbol{\varphi}_2), \quad \boldsymbol{\kappa} \stackrel{\text{def}}{=} \boldsymbol{\varphi}_2 - \boldsymbol{\varphi}_1. \quad (3.3)$$

where  $\mathbf{r} = \mathbf{r}_2 - \mathbf{r}_1$  is the vector connecting the particle centers of mass,  $\mathbf{r}_0$  is the value of  $\mathbf{r}$  in equilibrium,  $\boldsymbol{\varphi}_1$  and  $\boldsymbol{\varphi}_2$  are the vectors of small rotation of particles, and the coefficients  $\mathbf{A}$ ,  $\mathbf{B}$ , and  $\mathbf{C}$  are the coupling rigidity tensors. In the linear theory, the rigidity tensors are constant and can be calculated by the formulas [4]

$$\begin{aligned} \mathbf{A} &= - \sum_{k,n} \boldsymbol{\Psi}(\boldsymbol{\xi}_{kn}^0), & \mathbf{B} &= \frac{1}{2} \sum_{k,n} \boldsymbol{\Psi}(\boldsymbol{\xi}_{kn}^0) \times (\boldsymbol{\rho}_k + \boldsymbol{\rho}_n), \\ \mathbf{C} &= \frac{1}{2} \sum_{k,n} \left[ \frac{1}{2} \mathbf{r}_0 \times \boldsymbol{\Psi}(\boldsymbol{\xi}_{kn}^0) \times \mathbf{r}_0 + \boldsymbol{\rho}_k \times \boldsymbol{\Psi}(\boldsymbol{\xi}_{kn}^0) \times \boldsymbol{\rho}_n + \boldsymbol{\rho}_n \times \boldsymbol{\Psi}(\boldsymbol{\xi}_{kn}^0) \times \boldsymbol{\rho}_k \right], \end{aligned} \quad (3.4)$$

where  $\boldsymbol{\xi}_{kn}^0$  is the difference between the absolute position vectors of mass points belonging to different particles in the initial configuration and  $\boldsymbol{\rho}_n$  and  $\boldsymbol{\rho}_k$  are the position vectors of interacting mass points

determined in equilibrium with respect to the particle centers. The tensor  $\Psi(\boldsymbol{\xi})$  is determined on the basis of the interaction force,

$$\begin{aligned}\Psi(\boldsymbol{\xi}) &\stackrel{\text{def}}{=} \frac{d}{d\boldsymbol{\xi}} \mathbf{f}(\boldsymbol{\xi}) = 2\Phi'(\xi^2)\boldsymbol{\xi}\boldsymbol{\xi} + \Phi(\xi^2)\mathbf{E}, \\ \mathbf{f}(\boldsymbol{\xi}) &= \Phi(\xi_{kn}^2)\boldsymbol{\xi}_{kn}, \quad \Phi(\xi_{kn}^2) \stackrel{\text{def}}{=} -\frac{1}{\xi_{kn}}\Pi'(\xi_{kn}).\end{aligned}\quad (3.5)$$

Here  $\Pi$  is the interaction potential (in the present paper, we use the Lennard–Jones potential), and  $\mathbf{f}$  is the interaction force. In the case under study, the system has two orthogonal planes of symmetry, and therefore, the rigidity tensors can be represented in the form

$$\mathbf{A} = A_{11}\mathbf{i}\mathbf{i} + A_{22}\mathbf{j}\mathbf{j}, \quad \mathbf{B} = 0, \quad \mathbf{C} = C_{33}\mathbf{k}\mathbf{k}, \quad (3.6)$$

where the vectors  $\mathbf{i}$ ,  $\mathbf{j}$ ,  $\mathbf{k}$  form an orthonormal basis such that the vectors  $\mathbf{i}$ ,  $\mathbf{j}$  lie in the plane of the triangles and  $\mathbf{k}$  is perpendicular to this plane. We assume that the vector  $\mathbf{i}$  is directed along  $\mathbf{r}_0$ . By summing all interactions between the mass points forming the triangles, we find the rigidities of the couplings between the triangles:

$$\begin{aligned}A_{11} &= 2C_1 + C_4 + 4C_2 \cos^2 \alpha + 2C_3 \cos^2 \beta - (4\Phi_2 \sin^2 \alpha + 2\Phi_3 \sin^2 \beta), \\ A_{22} &= 4C_2 \sin^2 \alpha + 2C_3 \sin^2 \beta - (2\Phi_1 + \Phi_4 + 4\Phi_2 \cos^2 \alpha + 2\Phi_3 \cos^2 \beta), \\ C_{33} &= \frac{1}{4}A_{22}r_0^2 + (C_1 - C_4 + 2C_2 - 2C_3)l^2 + \frac{1}{2}l^2(C_1 + \Phi_1) + l^2(C_4 + \Phi_4) \\ &\quad + (C_3 + \Phi_3)l^2(\cos \beta - \sqrt{3} \sin \beta)^2 - 2l^2(C_2 + \Phi_2) \cos^2 \alpha, \\ C_i &\stackrel{\text{def}}{=} \Pi''(r_i), \quad \Phi_i \stackrel{\text{def}}{=} -\frac{\Pi'(r_i)}{r_i},\end{aligned}\quad (3.7)$$

where  $r_i$  are the distances between the mass points in the reference configuration and the angles  $\alpha$  and  $\beta$  between the couplings are defined in Fig. 2.

The system stability condition is the positive definiteness of the quadratic form (3.1). This condition is satisfied provided that the inequalities

$$A_{11} > 0, \quad A_{22} > 0, \quad C_{33} > 0 \quad (3.8)$$

hold. By substituting (3.7) into (3.8), we obtain a system of inequalities for the parameters  $\zeta$  and  $\eta$ . Further, by eliminating  $\eta$  from this system by formula (2.6), we obtain some restrictions imposed by the stability condition on the relative particle size  $\zeta$ . As a result, by numerically solving the inequalities thus obtained, we manage to show that system (3.8) can be reduced to the inequality  $A_{22} > 0$ , which implies the following stability condition for the two-particle system:

$$\zeta < \zeta_{\max} = 0.2303935. \quad (3.9)$$

Thus, the stability condition for the two-particle system implies an upper bound for the relative particle size; this bound is approximately as follows:

$$l < 0.23r_0. \quad (3.10)$$

#### 4. STABILITY OF A GRAPHENE LAYER. THE NEAREST NEIGHBOR APPROXIMATION

Consider a two-dimensional graphite lattice (graphene layer) formed by particles of the special shape. If only the interaction between nearest neighbors is taken into account, then the equilibrium equation leads to formula (2.5) and the distance between nearest neighbors in the lattice is equal to the distance between the centers of triangles in the system considered in the preceding section. Therefore, the relation between the size of and the distances between the triangles, obtained for two particles, can also be used for infinite sets of particles forming the graphene layer.

For a linear Cosserat continuum, the strain energy density can be represented as a quadratic form of the strain tensors [5]:

$$W = \frac{1}{2}\boldsymbol{\varepsilon}^T \cdot \cdot \mathbf{A} \cdot \cdot \boldsymbol{\varepsilon} + \boldsymbol{\varepsilon}^T \cdot \cdot \mathbf{B} \cdot \cdot \boldsymbol{\kappa} + \frac{1}{2}\boldsymbol{\kappa}^T \cdot \cdot \mathbf{C} \cdot \cdot \boldsymbol{\kappa}, \quad (4.1)$$

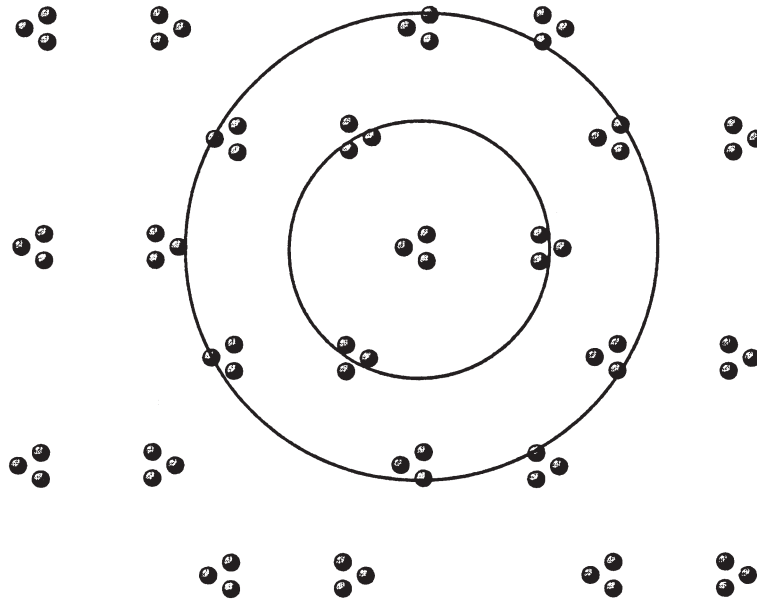


Fig. 3.

where  $W$  is the energy per unit volume,  $\mathbf{A}$ ,  $\mathbf{B}$ , and  $\mathbf{C}$  are the force, cross, and moment rigidity tensors, and  $\boldsymbol{\varepsilon}$  and  $\boldsymbol{\kappa}$  are the tension-shear and bending-torsion strain tensors determined by the formulas

$$\boldsymbol{\varepsilon} \stackrel{\text{def}}{=} \nabla \mathbf{u} + \mathbf{E} \times \boldsymbol{\varphi}, \quad \boldsymbol{\kappa} \stackrel{\text{def}}{=} \nabla \boldsymbol{\varphi}, \tag{4.2}$$

in which  $\mathbf{u}$  and  $\boldsymbol{\varphi}$  are the displacement and rotation of a medium element and  $\mathbf{E}$  is the unit tensor. We note that in the preceding section the symbols  $\boldsymbol{\varepsilon}$  and  $\boldsymbol{\kappa}$  were used to denote different strains, namely, vector strains realized at the microlevel.

The two-dimensional layer under study has rotation symmetry of order 3, and hence the corresponding elastic material is isotropic. Then the rigidity tensors can be written as [5]

$${}^4\mathbf{A} = A_1 \mathbf{J}_1 + A_2 \mathbf{J}_2 + A_3 \mathbf{J}_3, \quad {}^4\mathbf{B} = 0, \quad {}^4\mathbf{C} = \sqrt{3}C(\mathbf{ikki} + \mathbf{jkkj}), \tag{4.3}$$

where

$$\mathbf{J}_1 \stackrel{\text{def}}{=} \mathbf{e}_k \mathbf{e}_k \mathbf{e}_n \mathbf{e}_n, \quad \mathbf{J}_2 \stackrel{\text{def}}{=} \mathbf{e}_k \mathbf{e}_n \mathbf{e}_n \mathbf{e}_k, \quad \mathbf{J}_3 \stackrel{\text{def}}{=} \mathbf{e}_k \mathbf{e}_n \mathbf{e}_k \mathbf{e}_n \tag{4.4}$$

are isotropic tensors of rank 4, summation over repeated indices  $k$  and  $n$  is performed from 1 to 2,  $\mathbf{e}_1 = \mathbf{i}$ , and  $\mathbf{e}_2 = \mathbf{j}$ . The coefficients  $A_k$  for the case in which only neighboring particles interact in the crystal lattice (Fig. 3) were obtained in [5]:

$$\begin{aligned} A_1 &= \frac{\sqrt{3}}{12} r_0^2 \left[ A - D + \frac{(A - D)^2}{A + D} \right], \\ A_2 &= \frac{\sqrt{3}}{12} r_0^2 \left[ A + 3D - \frac{(A - D)^2}{A + D} \right], \\ A_3 &= \frac{\sqrt{3}}{12} r_0^2 \left[ A - D - \frac{(A - D)^2}{A + D} \right]. \end{aligned} \tag{4.5}$$

The longitudinal and transverse rigidity coefficients  $A$  and  $D$  and the torsional rigidity  $C$  are related to the above rigidities of interaction between the particles-triangles as follows:

$$Ar_0^2 = A_{11}, \quad Dr_0^2 = A_{22}; \quad C = C_{33}. \tag{4.6}$$

The material stability criterion is the positive definiteness of the quadratic form (4.1). Each summand in the quadratic form is independent, and hence we obtain the following two conditions:

$$\boldsymbol{\varepsilon}^T \dots {}^4\mathbf{A} \dots \boldsymbol{\varepsilon} > 0, \quad \boldsymbol{\kappa}^T \dots {}^4\mathbf{C} \dots \boldsymbol{\kappa} > 0. \tag{4.7}$$

We represent the strain tensors in the form

$$\boldsymbol{\varepsilon} = \varepsilon_{xx}\mathbf{ii} + \varepsilon_{xy}\mathbf{ij} + \varepsilon_{yx}\mathbf{ji} + \varepsilon_{yy}\mathbf{jj}, \quad \boldsymbol{\kappa} = \kappa_{xz}\mathbf{ik} + \kappa_{yz}\mathbf{jk}. \quad (4.8)$$

By substituting the first formula in (4.8) into (4.7), we obtain the inequality

$$A_1(\varepsilon_{xx}^2 + \varepsilon_{yy}^2 + 2\varepsilon_{xx}\varepsilon_{yy}) + A_2(\varepsilon_{xx}^2 + \varepsilon_{yy}^2 + \varepsilon_{xy}^2 + \varepsilon_{yx}^2) + A_3(\varepsilon_{xx}^2 + \varepsilon_{yy}^2 + 2\varepsilon_{xy}\varepsilon_{yx}) > 0, \quad (4.9)$$

where  $A_1$ ,  $A_2$ ,  $A_3$  are given by (4.5). This implies the four independent conditions

$$A_2 > 0, \quad A_2^2 - A_3^2 > 0, \quad A_1 + A_2 + A_3 > 0, \quad (A_1 + A_2 + A_3)^2 - A_1^2 > 0. \quad (4.10)$$

It follows from the stability conditions for a system of two interacting particles that the parameters  $A$  and  $D$  characterizing the longitudinal and transverse interaction rigidities are positive. Then the four inequalities in (4.10) are reduced to the two inequalities

$$A > D, \quad D > 0. \quad (4.11)$$

Numerical analysis shows that the first of these inequalities is satisfied for any  $\zeta$ . The second inequality can be reduced to the above inequality for the transverse rigidity of the coupling between the particles-triangles:  $A_{22} > 0$ . Thus, the microscopic consideration (the stability of two interacting particles) and the macroscopic consideration (the positive definiteness of the material strain energy) give the same results in the nearest neighbor approximation.

We take the second formula in (4.8) and substitute it into (4.7). This gives the condition

$$C(\kappa_{xz}^2 + \kappa_{yz}^2) > 0, \quad (4.12)$$

which is satisfied for all positive  $C = C_{33}$ .

## 5. SECOND-ORDER NEIGHBORS

The stability condition obtained above coincides with (3.8) and implies an upper bound for the particle size depending on the distance between the particles. The lower bound is zero. This means that infinitely small triangles, i.e., mass points, can be used. But, as a rule, the use of mass points as a model of particles cannot ensure stability of the lattice. The cause is that remote (second- and higher-order) neighbors are located on the unstable part of the “interaction force–distance” diagram, where the corresponding coupling rigidities are negative. At the same time, the couplings between nearest neighbors in the graphite lattice do not form a rigid structure; the lattice can be deformed with the lengths of these couplings remaining unchanged. For such deformations, stability is determined by the rigidities of further couplings, and since these couplings are negative, the material becomes unstable. Thus, it is insufficient to take into account only the nearest neighbors, because remote neighbors significantly affect the stability of the system. Consider the atoms belonging to the second coordination sphere. They lie at the distance  $b = \sqrt{3}r_0$  of the given atom (Fig. 3). We assume that the shear rigidity of the coupling with the remote neighbors is insignificant owing to their remoteness. Then the interaction with remote neighbors can be treated as interaction between mass points. The force balance equation has the form

$$\tilde{f}_1(r_0) + 2\sqrt{3}\tilde{f}_2(\sqrt{3}r_0) = 0, \quad (5.1)$$

where  $\tilde{f}_1(r_0)$  is the sum of all actions on the first coordination sphere. It coincides with the left-hand side of Eq. (2.5) for  $r = r_0$ . The term  $\tilde{f}_2(\sqrt{3}r_0)$  is responsible for the interaction with remote neighbors. Solving Eq. (5.1), we obtain the following relation (similar to (2.6)) for the case under study:

$$\eta^6 = \frac{\frac{1}{3^3} + \frac{1}{(1-\zeta)^7} + \frac{2+\zeta}{(1+\zeta+\zeta^2)^4} + \frac{1-\zeta}{[(1-\zeta)^2+3\zeta^2]^4} + \frac{1}{2(1+2\zeta)^7}}{\frac{1}{3^6} + \frac{1}{(1-\zeta)^{13}} + \frac{2+\zeta}{(1+\zeta+\zeta^2)^7} + \frac{1-\zeta}{[(1-\zeta)^2+3\zeta^2]^7} + \frac{1}{2(1+2\zeta)^{13}}}, \quad (5.2)$$

Using the approach proposed in [5], where the coefficients  $A_k$  are determined for the nearest neighbors, we find the rigidity tensors for our case:

$$\begin{aligned} A_1 &= \frac{\sqrt{3}}{12} r_0^2 \left[ A - D + 18B + \frac{(A - D)^2}{A + D + 6B} \right], \\ A_2 &= \frac{\sqrt{3}}{12} r_0^2 \left[ A + 3D + 18B - \frac{(A - D)^2}{A + D + 6B} \right], \\ A_3 &= \frac{\sqrt{3}}{12} r_0^2 \left[ A - D + 18B - \frac{(A - D)^2}{A + D + 6B} \right], \end{aligned} \quad (5.3)$$

where  $B < 0$  is the coupling rigidity coefficient for second-order neighbors. Now we use (5.2) to obtain stability conditions in the same way as in the case of nearest neighbors. Solving the inequalities (4.10) numerically in the case of the Lennard–Jones potential, we obtain

$$\zeta_{\min} < \zeta < \zeta_{\max}, \quad \zeta_{\min} = 0.0820795, \quad \zeta_{\max} = 0.2240461. \quad (5.4)$$

Thus, the material stability condition gives a two-sided constraint on the relative particle size, which can be written as

$$0.082r_0 < l < 0.224r_0, \quad (5.5)$$

where  $l$  is the effective particle size and  $r_0$  is the distance between the particle centers. Taking into account remote neighbors has permitted us to obtain a lower bound for the triangle size as well as an improved upper bound. This means that the suggested model allows one to stabilize the graphite lattice.

## 6. CONSTRUCTION OF THE GENERALIZED PAIR MOMENT POTENTIAL

The model proposed above permits one to stabilize the two-dimensional graphite lattice but is not fully consistent with the values of the graphite elastic moduli. According to [4], the ratio of the transverse rigidity coefficient  $D$  to the longitudinal rigidity coefficient  $A$  computed from experimental values of the elastic moduli is equal to 55%. We express the rigidities  $C_i$  via the parameter  $\zeta$  and use (3.7) to construct the ratio  $A_{22}/A_{11}$ . This ratio, which should be equal to  $D/A$ , is of the order of 2% within the stability region (5.5). This dramatic difference forces us to use the above model to construct different models with the desired rigidity ratio. The following two methods for constructing such models are possible: one takes another type of particles interacting via classical pair potentials or constructs a generalized interaction potential allowing for rotational degrees of freedom. In what follows, we consider the second method, which permits one to obtain a stable hexagonal lattice with a given longitudinal–transverse rigidity ratio.

Consider the general form of a moment potential capable of forming a hexagonal lattice on the plane [9, 10]:

$$U(R, \gamma, \kappa) = \Pi_0(r) + \Pi_1(r) \sin(n\gamma) \sin(n\kappa/2). \quad (6.1)$$

Here  $n$  is a parameter characterizing the symmetry order of the particle ( $n = 3$  for graphite),  $\Pi_0(r)$  is a momentless interaction potential of Lennard–Jones type, and  $\Pi_1(r)$  is a function of the distance  $r$  between the particles, which should tend to zero for large  $r$ . The rotational degrees of freedom are characterized by the shear angle  $\gamma$  and the relative rotation angle  $\varphi$ :

$$\gamma = \theta - \frac{1}{2}(\varphi_1 + \varphi_2), \quad \kappa = \varphi_2 - \varphi_1, \quad (6.2)$$

where the angles  $\varphi_i$  are responsible for the rotation of the  $i$ th particle about its center of mass and  $\theta$  is the angle determining the direction of the straight line connecting the particles. All the angles are counted from some fixed straight line. The interatomic coupling rigidities can be found by the formulas

$$A_{11} = U_r'', \quad A_{22} = \frac{1}{r^2} U_\gamma'', \quad C_{33} = U_\kappa'', \quad (6.3)$$

where the derivatives are calculated in the equilibrium  $r = r_0$ ,  $\kappa = \kappa_0$ ,  $\gamma = \gamma_0$ .

Formula (6.1) for the interaction potential was first obtained in [9] with the use of the triangle-atom model considered above. By expanding the potentials of interaction between the mass points into series in the small parameter  $\varepsilon = \zeta/\eta = l/\rho$ , the following formulas were obtained for  $\Pi_0(r)$  and  $\Pi_1(r)$  in [10]:

$$\begin{aligned}\Pi_0 &= 9D \left[ \left( \frac{\rho}{r} \right)^{12} - 2 \left( \frac{\rho}{r} \right)^6 \right] + 324D \left[ 2 \left( \frac{\rho}{r} \right)^{14} - \left( \frac{\rho}{r} \right)^8 \right] \left( \frac{l}{\rho} \right)^2, \\ \Pi_1 &= 144D \left[ -14 \left( \frac{\rho}{r} \right)^{15} + 5 \left( \frac{\rho}{r} \right)^9 \right] \left( \frac{l}{\rho} \right)^3\end{aligned}\quad (6.4)$$

where  $l$  is the characteristic size of the triangle and  $\rho$  is the interaction range. We express the known coupling rigidities via the parameter  $\zeta = l/r_0$  in the same way as in the preceding sections and obtain the stability domain

$$0.092r_0 < l < 0.265r_0, \quad (6.5)$$

similar to (5.5), where  $r_0$  is the interatomic distance in the equilibrium configuration. By equating the interaction rigidity ratio to the well-known value for graphite [5, 8],

$$\frac{A_{11}}{A_{22}} = 2.1, \quad (6.6)$$

we determine the relative particle size

$$\zeta = 0.27; \quad (6.7)$$

i.e., the value of the parameter  $\zeta$  in this case lies in the stability domain (6.5).

The potential studied in [9] was constructed under the assumption that  $\varepsilon$  is small, and hence it can be successfully used in the case of large interatomic distances. But for small distances this approximation does not work, which leads to various undesirable effects, including loss of stability. In numerical simulation, for example, by the molecular dynamic method, it is necessary to construct a moment interaction potential that can be used on the entire range of simulation, from infinitely small to infinitely large distances between particles.

For the specific form of the potential (6.1) for modeling the graphite lattice, we take the potential

$$U(r, \gamma, \kappa) = D_1 \left[ \left( \frac{\rho}{r} \right)^{12} - 2 \left( \frac{\rho}{r} \right)^6 \right] + D_2 \left( \frac{\rho}{r} \right)^m \sin(3\gamma) \sin\left( \frac{3\kappa}{2} \right). \quad (6.8)$$

The coefficient  $D_2$  is responsible for the moment contribution into the interaction between the particles. (For  $D_2 = 0$ , the potential (6.8) coincides with the Lennard–Jones potential.) The introduction of this coefficient permits one to omit the dependence of the potential on the particle size. Now let us study the stability of a system of two neighboring atoms. The radial and transverse components  $F_r$  and  $F_\theta$  of the force vector and the value  $M^C$  of the moment vector with respect to the midpoint of the segment connecting the particles are calculated by the formulas

$$F_r = \frac{\partial U}{\partial r}, \quad F_\theta = \frac{1}{r} \frac{\partial U}{\partial \theta}, \quad M^C = \frac{\partial U}{\partial \kappa}. \quad (6.9)$$

In an equilibrium, all force components should be zero. Thus, we can calculate the equilibrium angles  $\gamma_0$  and  $\kappa_0$  as well as the equilibrium distance  $r_0$  between the particles as a function of the coefficients  $D_1$  and  $D_2$ . The coupling rigidity coefficients can be determined from (6.3). In a stable equilibrium, the coupling rigidities expressed as functions of  $D_1$  and  $D_2$  should be positive. In their structure, they are similar to (3.8), but the coefficients  $A_{22}$  and  $C_{33}$  differ only by a positive factor; therefore, we have only two rather than three independent stability conditions.

We consider the case  $m = 12$  by analogy with the Lennard–Jones potential. Then

$$r_0 = \rho \left( 1 + \frac{D_2}{D_1} \right)^{1/6}, \quad (6.10)$$

The conditions  $A_{11}, A_{22} > 0$  and relation (6.6) for the rigidities result in the system

$$\frac{D_1}{D_2} = -1.26, \quad D_2 < 0, \quad (6.11)$$



We assume that the equilibrium distance between the particles is equal to the interatomic distance in the graphite lattice; then  $r_0 = 0.142$  nm. Using formula (6.10), we calculate the parameter  $\rho$  of the Lennard–Jones potential. Knowing  $\rho$  and  $r_0$  and using the value  $A_{11} = 730$  N/m [5], from (6.3) and (6.11) we obtain the parameter values

$$\rho = 0.184 \text{ nm}, \quad D_1 = 0.266 \text{ eV}, \quad D_2 = -0.210 \text{ eV}. \quad (6.12)$$

Thus, we have obtained the potential which, without determining the shape and size of the particles, allows us to describe stable interaction between carbon atoms in the graphite lattice for various interatomic distances.

## 7. CONCLUSION

In the present paper, we present a mechanical model describing a two-dimensional hexagonal crystal lattice. We show that the pair moment interaction can ensure stability of such a lattice. We find the stability domain depending on the ratio of the characteristic size of particles of special type to the distance between them. We also show that the upper bound of the stability domain is related to the stability of the total atom–particle interaction. The lower bound characterizes the balance between the stabilizing moment interaction of first-order neighbors and the destabilizing force interaction between second-order neighbors. This balance is essential for particles of small characteristic size. Thus, this model permits one to ensure stability of the graphite lattice. But computations show that this model gives a strongly underestimated value of the transverse-to-longitudinal coupling rigidity ratio. To solve this problem, in the present paper we propose a generalized moment potential describing the interaction of particles of general shape, which permits one to deal with a rigidity ratio that is in good agreement with experiments. The results obtained in this paper can be used in both theoretical computations and computer simulation of carbon nanosystems.

## ACKNOWLEDGMENTS

The research was supported by the Russian Foundation for Basic Research (project no. 05-01-00094-a).

## REFERENCES

1. J. Tersoff, “New Empirical Approach for the Structure and Energy of Covalent Systems,” *Phys. Rev. B* **37**, 6991–7000 (1988).
2. D. W. Brenner, “Empirical Potential for Hydrocarbons for Use in Simulating the Chemical Vapor Deposition of Diamond Films,” *Phys. Rev. B* **42**, 9458–9471 (1990).
3. A. M. Krivtsov, *Deformation and fracture of solids with microstructure* (Fizmatlit, Moscow, 2007) [in Russian].
4. E. A. Ivanova, A. M. Krivtsov, N. F. Morozov, and A. D. Firsova, “Description of Crystal Packing of Particles with Torque Interaction,” *Izv. Akad. Nauk. Mekh. Tverd. Tela*, No. 4, 110–127 (2003) [Mech. Solids (Engl. Transl.)].
5. E. A. Ivanova, A. M. Krivtsov, and N. F. Morozov, “Obtaining Macroscopic Elasticity Relations for Complex Crystal Lattices with Moment Interactions Taken into Account at the Microlevel,” *Prikl. Mat. Mekh.* **71** (4), 595–615 (2007) [J. Appl. Math. Mech. (Engl. Transl.)].
6. R. V. Goldstein and A. V. Chentsov, “Discrete-Continuum Model of a Nanotube,” *Izv. Akad. Nauk. Mekh. Tverd. Tela*, No. 4, 57–74 (2005) [Mech. Solids (Engl. Transl.)].
7. I. S. Pavlov, “Elastic Waves in a 2D Granular Medium,” in *Problems of Strength and Plasticity. Collection of VUZ papers* (Nizhniy Novgorod State University Press, Nizhnii Novgorod, 2005), No. 67, pp. 119–131 [in Russian].
8. V.A. Gorodtsov and D. S. Lisovenko, “Elastic Properties of Graphite Rods and Multiwalled Carbon Nanotubes (Torsion and Extension),” *Izv. Akad. Nauk. Mekh. Tverd. Tela*, No. 4, 42–56 (2005) [Mech. Solids (Engl. Transl.)].
9. A. P. Byzov and E. A. Ivanova, “Mathematical Simulation of Moment Interactions of Particles with Rotational Degrees of Freedom,” *Naučno-tehnicheskie vedomosti SPbGPU*, No. 2 (2007).
10. A. P. Byzov and E. A. Ivanova, “Interaction Potentials for Particles with Rotational Degrees of Freedom,” in *Modern Problems of Continuum Mechanics. Proc. IXth International Conference Dedicated to Academician I. I. Vorovich on the Occasion of His 85th Birthday, Rostov-on-Don, October 2005* (TsVVR, Rostov-on-Don, 2006), Vol. 2, pp. 47–51 [in Russian].